Preparation and Photophysical Properties of *Bis*(tridentate) Iridium(III) Emitters: Pincer Coordination of 2,6-Di(2-pyridyl)phenyl

Pierre-Luc T. Boudreault,[b] Miguel A. Esteruelas,[a] Daniel Gómez-Bautista,[a] Susana Izquierdo,[a] Ana M. López,[a] Enrique Oñate,[a] Esther Raga,[a] Jui-Yi Tsai[b]*

[a]Departamento de Química Inorgánica – Instituto de Síntesis Química y Catálisis Homogénea (ISQCH) – Centro de Innovación en Química Avanzada (ORFEO-CINQA), Universidad de Zaragoza – CSIC, 50009 Zaragoza, Spain

[b]Universal Display Corporation, 375 Phillips Boulevard, Ewing, New Jersey 08618, USA

ABSTRACT: The way to prepare molecular emitters [5t + 4t'] of iridium(III) with a 5t ligand derived from the abstraction of the hydrogen atom at position 2 of the aryl group of 1,3-di(2-pyridyl)benzene (dpybH) is shown. In addition, the photophysical properties of the new emitters are compared with those of their counterparts resulting from the deprotonation of 1,3-di(2-pyridyl)-4,6-dimethylbenzene (dpyMebH), at the same position, which are also synthetized. Treatment of 0.5 equiv of the dimer $[Ir(\mu\text{-}Cl)(\eta^2\text{-}COE)_2]_2$ (COE = cyclooctene) with 1.0 equiv of

Hg(dpyb)Cl leads to the iridium(III) derivative $IrCl_2\{\kappa^3\text{-}N,C,N\text{-}(dpyb)\}(\eta^2\text{-}COE)$ (**3**), which reacts with 2-(1*H*-imidazol-2-yl)-6-phenylpyridine ($HNImpyC_6H_5$) and 2-(1*H*-benzimidazol-2-yl)-6-phenylpyridine ($HNBzimpyC_6H_5$) in the presence of Na_2CO_3 to give $Ir\{\kappa^3\text{-}C,N,N\text{-}(NImpyC_6H_4)\}\{\kappa^3\text{-}N,C,N\text{-}(dpyb)\}$ (**4**) and $Ir\{\kappa^3\text{-}C,N,N\text{-}(NBzimpyC_6H_4)\}\{\kappa^3\text{-}N,C,N\text{-}(dpyb)\}$ (**5**), respectively. Similar reactions of the Williams' dimer $[IrCl(\mu\text{-}Cl)\{\kappa^3\text{-}N,C,N\text{-}(dpyMeb)\}]_2$ with $HNImpyC_6H_5$ and $HNBzimpyC_6H_5$ in the presence of Na_2CO_3 afford the dimethylated counterparts $Ir\{\kappa^3\text{-}C,N,N\text{-}(NImpyC_6H_4)\}\{\kappa^3\text{-}N,C,N\text{-}(dpyMeb)\}$ (**6**) and $Ir\{\kappa^3\text{-}C,N,N\text{-}(NBzimpyC_6H_4)\}\{\kappa^3\text{-}N,C,N\text{-}(dpyMeb)\}$ (**7**), whereas 2-(6-phenylpyridine-2-yl)-1*H*-indole ($HIndpyC_6H_5$) initially gives $IrH\{\kappa^2\text{-}N,N\text{-}(IndpyC_6H_5)\}\{\kappa^3\text{-}N,C,N\text{-}(dpyMeb)\}$ (**8**) and subsequently $Ir\{\kappa^3\text{-}C,N,N\text{-}(IndpyC_6H_4)\}\{\kappa^3\text{-}N,C,N\text{-}(dpyMeb)\}$ (**9**). Complexes **4**–**7** are phosphorescent green emitters (λ_{em} 490–550 nm), whereas **9** is greenish yellow emissive (λ_{em} 547–624 nm). They display lifetimes in the range 0.5–9.7 μs and quantum yields in both doped poly(methyl)methacrylate films and in 2-methyltetrahydrofuran at room temperature depending upon the ligands: 0.5–0.7 for **6** and **7**, about 0.4 for **4** and **5**, and 0.3–0.2 for **9**.

Introduction

Pincer-transition metal complexes are having a tremendous impact in the current chemistry because of the broad range of their applications, including material science.[1] For instance, their use is allowing to design new families of phosphorescent emitters and to improve the stability and photophysical properties of other ones already known.[2] Although the structural distortions induced by rigidity of these ligands was initially considered a problem for the emission efficiency,[3] it was soon noted that the increase in strength of the metal-ligand binding, due to the triple interaction, may have a positive effect on the thermal induced quenching.[4] In addition,

pincer ligands allow to reduce the number of groups at the metal coordination sphere, with regard to bidentate and monodentate ligands, for a given coordination index. This prevents issues of structural isomers and redistribution reactions on heteroleptic emitters with different ligands.[5]

Phosphorescent iridium(III) molecules are at the forefront of photophysics[6] and photochemistry.[7] However, complexes of this class stabilized by two different tridentate ligands (t), one of them monoanionic 5e donor (5t) and the other dianionic 4e donor (4t'), are very scarce.[2] This is in part due to the lack of synthesis pathways of broad applicability.

1,3-Di(2-pyridyl)benzene (dpybH) was implied in the early attempts to build iridium(III) [5t + 4t'] emitters.[8] Inspired in previous work on ruthenium(II), osmium(II), and platinum(II),[9] in 2004, Williams and co-workers performed the reaction of this organic molecule with $IrCl_3 \cdot 3H_2O$, under a wide range of conditions. However, the pyridyl-assisted activation of the phenyl C-H bond at position 4 took place, to generating a bidentate coordination instead of the desired pincer.[10] They reasoned that this binding mode could be blocked by introduction of substituents in the phenyl ring at positions 4 and 6. Thus, 1,3-di(2-pyridyl)-4,6-dimethylbenzene (dpyMebH) was synthetized, which successfully reacted with $IrCl_3 \cdot 3H_2O$ in 2-ethoxyethanol to afford the dinuclear complex $[IrCl(\mu\text{-}Cl)(dpyMeb)]_2$ bearing the desired pincer.[11] This complex has been used as a source of the 5t ligand and precursor of the [5t + 4t'] emitters, by several research groups, since it allows the easy coordination of a 4t' ligand in basic medium (Scheme 1).[10-12]

Scheme 1. Preparation of a [5t + 4t'] Ir(III) Complex via Williams' Dimer[10,11]

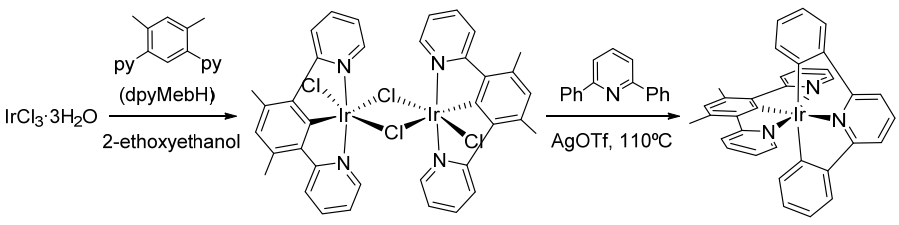

The success of Williams has strongly influenced the [5t + 4t'] emitters prepared until very recently. While a variety of 4t ligands has been used, the 5t group has been mainly focused on modifications of dpyMebH.[12a] On the other hand, dpybH has been rejected as a source of 5t pincers.

A notable effort is being carried out to increase the variety of 5t ligands, in recent years. Some months ago, we described a straightforward synthetic route to prepare a dinuclear [IrCl(μ-Cl)(5t)]$_2$ complex, related to the Williams' dimer, which bears a 1,3-*bis*(imidazolylidene)phenyl group instead of dpyMeb. This compound allowed us to synthetize green and greenish yellow emitters by reaction with 2-(1*H*-imidazol-2-yl)-6-phenylpyridine (HNImpyC$_6$H$_5$) and 2-(1*H*-benzimidazol-2-yl)-6-phenylpyridine (HNBzimpyC$_6$H$_5$) in the presence of Na_2CO_3 (Scheme 2).[13] The procedure used to form the dimer is an extension of that developed to synthetize iridium(III) [6tt + 3b] blue-green emitters, where 6tt is a dianionic *C*,*C*,*C*,*C*-tetradentate ligand bearing two aryl-NHC moieties and 3b is an orthometalated phenyl-pyridine.[14] Previously, between 2016 and 2018, Chi, Chou and co-workers had synthetized interesting [5t + 4t'] emitters also bearing a 1,3-*bis*(imidazolylidene)phenyl ligand, while the other pincer-component of the structure contains at least a functionalized pyrazolate group. In contrast to that shown in Scheme 2, their synthesis was performed by one-pot procedures.[15] In the context of this class of emitters, it should be pointed out that ligands 4t'containing a 2-pyridyl-azolate moiety are attracting notable interest due to the σ-donor ability of the azolate, which along with the π-acceptor capacity of the pyridyl group, seem to afford a remarkable electron delocalization over the resulting five-membered heterometalacycle.[13,15,16]

Scheme 2. Preparation of [5t + 4t'] Ir(III) Complexes Bearing a 1,3-*Bis*(imidazolylidene)phenyl Group as 5t Ligand[13]

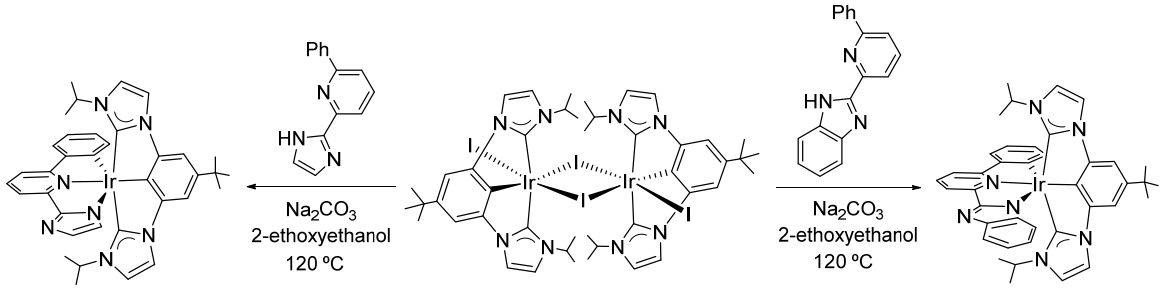

The HOMO of the [5t + 4t'] emitters shown in Scheme 2 mainly comprises the metal and the 5t and 4t' ligands, whereas the LUMO is mainly centered on π^* orbitals of the 4t' ligand.[13] Thus, the nature of the 5t group, including its substituents, plays a critical role in the HOMO-LUMO gap and therefore in the photophysical properties of the emitters; i.e., in principle, it should not be the same $^{i}PrImC_6H_2(5\text{-}^{t}Bu)Im^{i}Pr$ as dpyMeb or dpyb, from the point of view of the photophysical properties. In this context, it should be noted that, the quantum yield of the homoleptic emitter Ir{κ^2-*C*,*N*-(pyC_6H_4)}$_3$ is higher than that of the methyl-substituted Ir{κ^2-*C*,*N*-(pyC_6H_3Me)}$_3$. In addition, the substitution gives rise to a red-shift of the emission.[17] This fact and our interest by ligands 4t' containing a 2-pyridyl-azolate moiety[13,18] prompted us to prepare the dpyb and dpyMeb counterparts of the $^{i}PrImC_6H_2(5\text{-}^{t}Bu)Im^{i}Pr$-emitters shown in Scheme 2, for comparison purposes. Of course, we kept in mind that the first challenge should be to find a procedure to coordinate the dpyb ligand as a pincer. In this paper, we report a synthetic procedure to prepare a useful complex to obtain [5t + 4t'] emitters with a dpyb ligand as the 5t component of the structure, the synthesis of the target emitters, and their photophysical properties.

Results and Discussion

Pincer Coordination of dpyb to Iridium(III). Williams seems to be of the opinion that the central ion decides the reactivity of dpybH and therefore the coordination mode of the dpyb ligand. Whilst ruthenium(II), osmium(II), and platinum(II) afford a *N*,*C*,*N*-pincer binding mode, iridium(III), rhodium(III) and palladium(II) favor its bidentate coordination.[8] However, we note that although the C-H activation of the phenyl ring at positions 4 and 6 is kinetically favored with regard to the activation at position 2, by steric reasons, there is not a clear thermodynamic preference by the bidentate coordination with regard to the pincer. As a consequence, the nature of the formed compound strongly depends on the performed reaction; for a given ion, different types of complexes can be obtained. For instance, Cárdenas and Echavarren have reported that $Pd(OAc)_2$ promotes the double activation of the phenyl ring, whereas dpybH only undergoes pyridine coordination when $[PdCl_4]^{2-}$ is used instead of $Pd(OAc)_2$.[19] On the other hand, Soro, Stoccoro, Manassero, and co-workers have shown that the treatment of $Pd(OAc)_2$ with the organomercury(II) Hg(dpyb)Cl and LiX (X = Cl, Br, I) in ethanol affords Pd{κ^3-*N*,*C*,*N*-(dpyb)}X displaying *N*,*C*,*N*-pincer coordination of the dpyb ligand.[20]

We inspired in the work of Soro, Stoccoro, Manassero and co-workers to address the challenge of coordinating the dpyb ligand to iridium(III) in a *N*,*C*,*N*-pincer manner. We initially attempted the transmetalation of the ligand from the organomercury derivative to $IrCl_3 \cdot 3H_2O$, in order to prepare a dimer similar to that of Williams with dpyMeb. Treatment of 1.0 equiv of $IrCl_3 \cdot 3H_2O$ with 1.2 equiv of Hg(dpyb)Cl, in 2-ethoxyethanol/water (3:1) at 80 ºC, for 24 h leads to an orange solid, which corresponds to the desired dinuclear complex [IrCl(μ-Cl){κ^3-*N*,*C*,*N*-(dpyb)}]$_2$ (**1**), according to its C,N,H elemental analysis (Scheme 3). Although this dimer is obtained in high yield (70%), it is extremely insoluble in the usual organic solvents. We were

only able to dissolve it in dimethyl sulfoxide, at 80ºC. Under these conditions, the mononuclear species $IrCl_2\{\kappa^3\text{-}N,C,N\text{-}(dpyb)\}\{\kappa\text{-}S\text{-}(DMSO)\}$ (**2**) is formed (23%), but unfortunately the major amount of the dimer decomposes to unidentified products.

Scheme 3. Preparation of Dimer 1 Bearing dpyb as Pincer Ligand

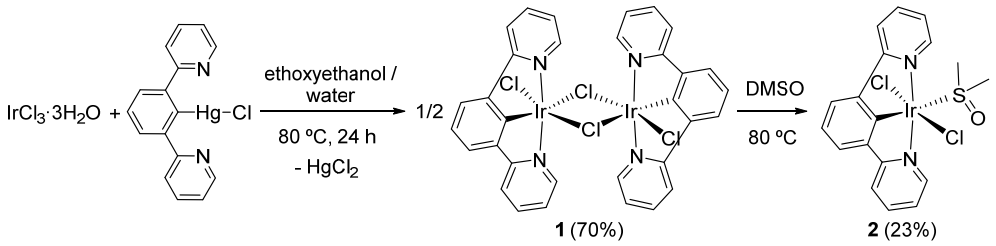

Complex **2** was isolated as a yellow solid and characterized by X-ray diffraction analysis. The structure (Figure 1) proves the pincer coordination of the dpyb ligand. The polyhedron around the iridium(III) center can be described as a distorted octahedron with *trans* chlorides (Cl(1)-Ir-Cl(2) = 178.99(2)º). The perpendicular plane is formed by the *N*,*C*,*N*-pincer, which acts with N(1)-Ir-N(2), N(1)-Ir-C(1), and N(2)-Ir-C(1) angles of 159.05(8), 79.50(9), and 79.55(9)º, respectively, and the dimethyl sulfoxide molecule coordinated by the sulfur atom and disposed *trans* to the metalated carbon atom of the aryl linker (S(1)-Ir-C(1) = 177.94(7)º). In agreement with the S-bonding,[21] the IR spectrum of the compound contains a ν(S-O) band at 1011 cm^{-1}, which is consistent with a S(1)-O(2) bond length of 1.4920(18) Å. The distance Ir-C(1) between the metal center and the metalated atom of the aryl group is 1.952(2) Å. A signal at 165.2 ppm, corresponding to the metalated C(1) atom, in the $^{13}C\{^1H\}$ NMR spectrum is other characteristic feature of **2**.

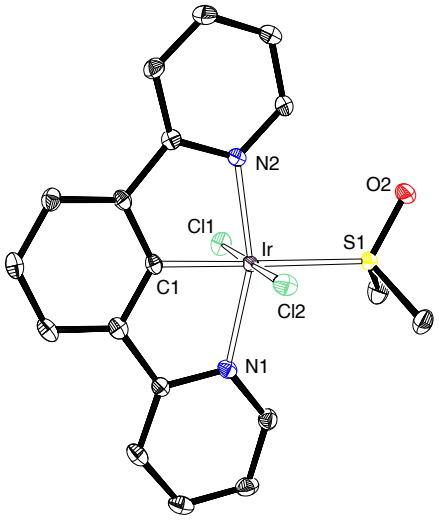

Figure 1. Molecular diagram of complex **2** (50% probability ellipsoids). Hydrogen atoms are omitted for clarity. Selected bond lengths (Å) and angles (deg): Ir-C(1) = 1.952(2), Ir-N(1) = 2.0873(19), Ir-N(2) = 2.0772(19), Ir-Cl(1) = 2.3605(6), Ir-Cl(2) = 2.3533(6), Ir-S(1) = 2.4380(6), S(1)-O(2) = 1.4920(18); N(1)-Ir-N(2) = 159.05(8), N(1)-Ir-C(1) = 79.50(9), N(2)-Ir-C(1) = 79.55(9), Cl(1)-Ir-Cl(2) = 178.99(2), C(1)-Ir-S(1) = 177.94(7).

Complexes **1** and **2** demonstrate that the dpyb ligand can also coordinate in a pincer fashion to iridium(III). However the insolubility of **1** prevents its use as a useful source of a 5t group. In this context, it should be mentioned that the well-known complex $[Ir(\mu\text{-Cl})(\eta^2\text{-COE})_2]_2$ is a usual alternative to $IrCl_3{\cdot}3H_2O$ to the preparation of homoleptic and heteroleptic dinuclear complexes $[Ir(\mu\text{-Cl})(3b)_2]_2$ and $[Ir(\mu\text{-Cl})(3b)(3b')]_2$, respectively,[5a,22] which are the entry to *tris*-bidentate-iridium(III) emitters. This precedent prompted us to attempt the transmetalation of dpyb from Hg(dpyb)Cl to the iridium(I) center of the iridium-olefin dimer. The addition of 1.0 equiv of the organomercury compound to 0.5 equiv of the dimer, in tetrahydrofuran, at room temperature led to the iridium(III) derivative $IrCl_2\{\kappa^3\text{-}N,C,N\text{-(dpyb)}\}(\eta^2\text{-COE})$ (**3**), as a result of a mercury-to-iridium transfer of the dpyb and chloride ligands (Scheme 4). The process involves the rupture of

the chloride bridge of [Ir(μ-Cl)(η^2-COE)$_2$]$_2$ and the oxidation of the iridium center. The change from iridium(I) to iridium(III) is accompanied by the reduction from mercury(II) to mercury(0).

Scheme 4. Preparation of Complex 3

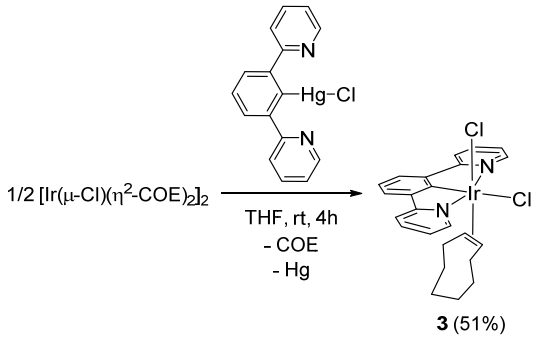

3 (51%)

Complex **3** was isolated as a yellow solid in 51% yield and characterized by X-ray diffraction analysis. Figure 2 shows a view of the structure, which is a new evidence for a pincer coordination of the dpyb ligand to iridium(III). The coordination polyhedron around the iridium center is the expected distorted octahedron with the *N*,*C*,*N*-ligand coordinated *mer* with N(1)-Ir-N(2), N(1)-Ir-C(1), and N(2)-Ir-C(1) angles of 157.7(5), 79.3(7), and 80.6(7)º, respectively. The phenyl linker is disposed *trans* to one of the chloride ligands (C(1)-Ir-Cl(2) =175.5(5)º), which lie mutually *cis* (Cl(1)-Ir-Cl(2) = 87.37(14)º), in contrast to that observed in **2**. The other one is disposed *trans* to the olefin, which coordinates in a symmetric manner (Ir-C(17) = Ir-C(18) = 2.243(18) Å). The coordination enlarges the olefin C(17)-C(18) bond until 1.40(2) Å. The distance between the metal center and the metalated atom of the aryl group of 1.932(16) Å (Ir-C(1)) compares well with that of **2**. The coordinated carbon atoms give rise to signals at 166.9 (C(1)) and 89.8 (C(17) and C(18)) ppm in the $^{13}C\{^1H\}$ NMR spectrum, in dichloromethane-d_2, at room temperature.

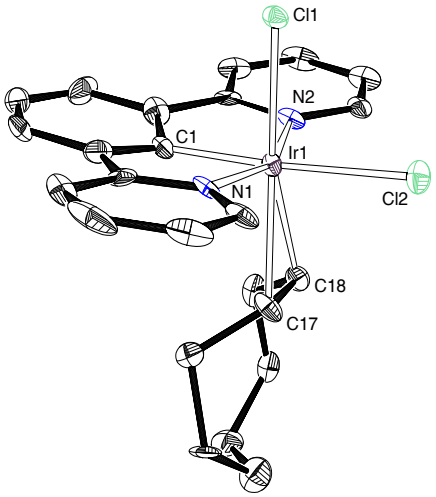

Figure 2. Molecular diagram of complex **3** (50% probability ellipsoids). Hydrogen atoms are omitted for clarity. Selected bond lengths (Å) and angles (deg): Ir-C(1) = 1.932(16), Ir-N(1) = 2.082(13), Ir-N(2) = 2.068(13), Ir-Cl(1) = 2.376(4), Ir-Cl(2) = 2.491(4), Ir-C(17) = 2.243(18), Ir-C(18) = 2.243(18), C(17)-C(18) = 1.40(2); N(1)-Ir-N(2) = 157.7(5), N(1)-Ir-C(1) = 79.3(7), N(2)-Ir-C(1) = 80.6(7), C(1)-Ir-Cl(2) = 175.5(5), Cl(1)-Ir-Cl(2) = 87.37(14).

Preparation of the [5t + 4t'] Emitters. Complex **3** is certainly useful to prepare [5t + 4t'] emitters with dpyb as a 5t group, in contrast to **1** and **2**. Its treatment with 1.0 equiv of $HNImpyC_6H_5$ and 5.0 equiv of sodium carbonate, in 2-ethoxyethanol, at 135ºC, for 3 days leads to the desired target compound Ir{κ^3-*C*,*N*,*N*-($NImpyC_6H_4$)}{κ^3-*N*,*C*,*N*-(dpyb)} (**4**), which was isolated as a yellow solid in 24% yield after the purification of the reaction crude by column chromatography. Under the same conditions the reaction of **3** with $HNBzimpyC_6H_5$ affords the related compound Ir{κ^3-*C*,*N*,*N*-($NBzimpyC_6H_4$)}{κ^3-*N*,*C*,*N*-(dpyb)} (**5**) in 14% yield (Scheme 5a). The dpyMeb-counterparts, Ir{κ^3-*C*,*N*,*N*-($NImpyC_6H_4$)}{κ^3-*N*,*C*,*N*-(dpyMeb)} (**6**) and Ir{κ^3-*C*,*N*,*N*-($NBzimpyC_6H_4$)}{κ^3-*N*,*C*,*N*-(dpyMeb)} (**7**), were similarly prepared by reaction of the Williams' dimer [IrCl(μ-Cl){κ^3-*N*,*C*,*N*-(dpyMeb)}]$_2$ with $HNImpyC_6H_5$ and $HNBzimpyC_6H_5$,

respectively, in the presence of sodium carbonate. Complexes **6** and **7** were obtained in higher yields, 55–58%, than compounds **4** and **5**, also as yellow solids (Scheme 5b).

Scheme 5. Preparation of Complexes 4–7

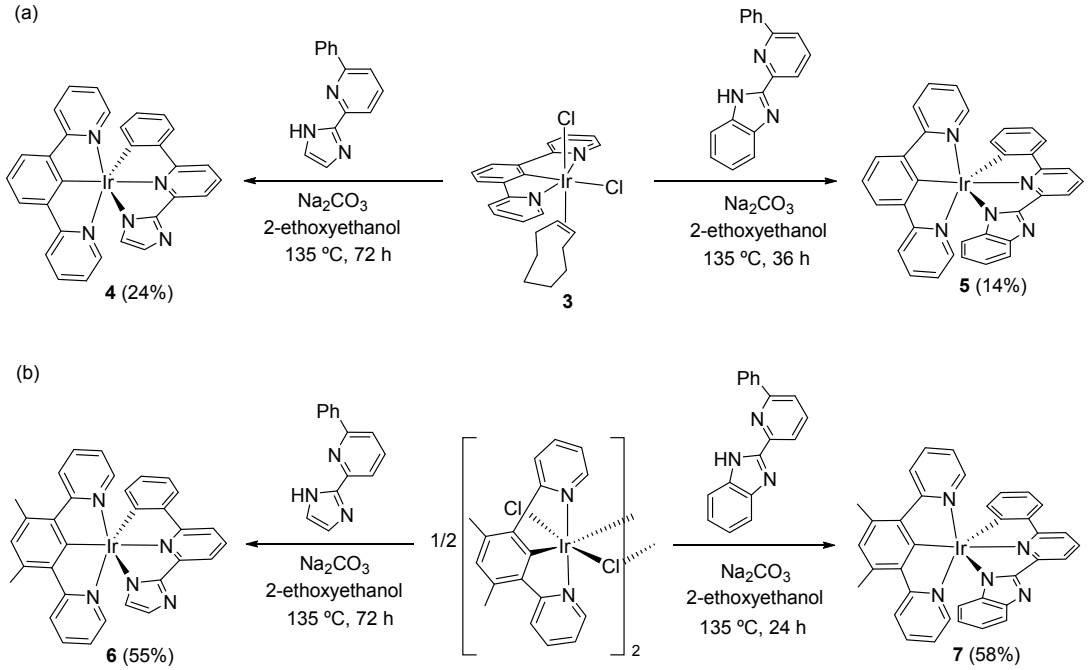

The formation of the target compounds was confirmed by means of the X-ray diffraction analysis of single crystals of **6** and **7**. Figures 3 and 4 show a view of the molecules. The coordination of both pincers around each iridium center gives rise to distorted octahedrons with N(4)-Ir-N(5), C(21)-Ir-N(1), and C(1)-Ir-N(2) angles of 160.3(3), 176.0(3), and 155.8(3)º for **6** and 160.09(11), 177.70(13), and 156.22(13)º for **7**. The iridium-aryl$_{5t}$ bond length, Ir-C(21), of 1.931 (8) Å for **6** and 1.938 (3) Å for **7** compare well with those of **2** and **3** and are about 0.1 Å shorter than the iridium-aryl$_{4t'}$ distance, Ir-C(1), of 2.043(10) Å for **6** and 2.023(3) Å for **7**. In the $^{13}C\{^{1}H\}$ NMR spectra of **4**–**7**, the resonance corresponding to the metalated carbon atom of the 5t ligand appears between 190 and 185 ppm, whereas that due to the 4t' group is observed between 148 and 146 ppm.

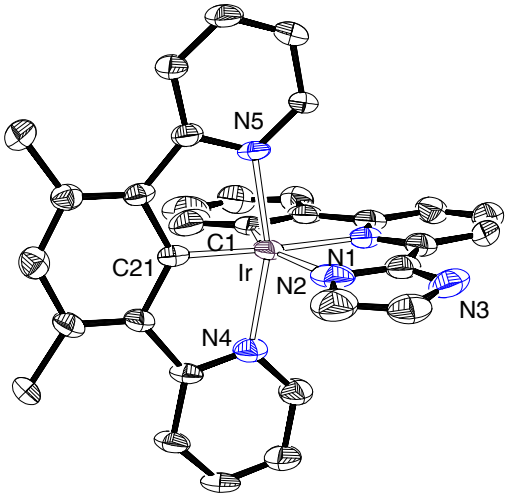

Figure 3. Molecular diagram of complex **6** (50% probability ellipsoids). Hydrogen atoms are omitted for clarity. Selected bond lengths (Å) and angles (deg): Ir-C(21) = 1.931(8), Ir-N(4) = 2.048(6), Ir-N(5) = 2.042(6), Ir-C(1) = 2.043(10), Ir-N(1) = 2.065(7), Ir-N(2) = 2.116(8); C(1)-Ir-N(2) = 155.8(3), N(4)-Ir-N(5) = 160.3(3), N(1)-Ir-C(21) = 176.0(3).

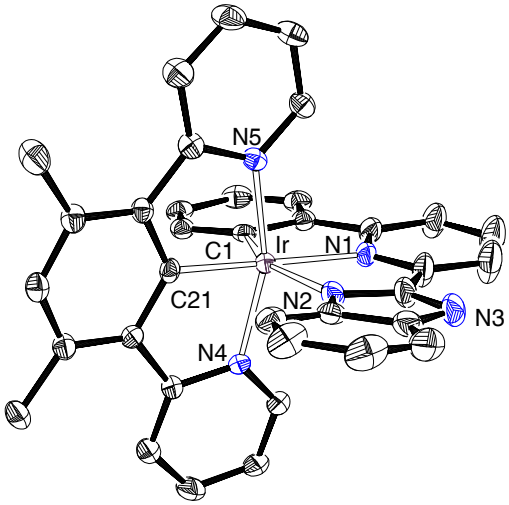

Figure 4. Molecular diagram of complex **7** (50% probability ellipsoids). Hydrogen atoms are omitted for clarity. Selected bond lengths (Å) and angles (deg): Ir-C(1) = 2.023(3), Ir-N(1) = 2.075(3), Ir-N(2) = 2.134(3), Ir-C(21) = 1.938(3), Ir-N(4) = 2.038(3), Ir-N(5) = 2.045(3),; C(1)-Ir-N(2) = 156.22(13), N(4)-Ir-N(5) = 160.09(11), N(1)-Ir-C(21) = 177.70(13).

We are also interested in learning about the influence of the free nitrogen atom of the heterocyclic substituent of the pyridine ring of the 4t' ligand on the photophysical properties of these [5t + 4t'] emitters. So, we decided to replace the benzimidazole moiety of HNBzimpyC_6H_5 by indole and to carry out the reaction of the resulting 2-(6-phenylpyridine-2-yl)-1*H*-indole (HIndpyC_6H_5) with the William's dimer. Preparations of the desired emitter proved to be very complicated and elaborate, needing two steps and potasium *tert*-butoxide, a stronger base than carbonate (Scheme 6). Treatment of 0.5 equiv of complex [IrCl(μ-Cl){κ^3-*N*,*C*,*N*-(dpyMeb)}]$_2$ with 1.0 equiv of HIndpyC_6H_5 and 2.5 equiv of KO^{t}Bu, in 2-ethoxyethanol at 110 ºC, for 14 h initially leads to the hydride derivative IrH{κ^2-*N*,*N*-(IndpyC_6H_5)}{κ^3-*N*,*C*,*N*-(dpyMeb)} (**8**), which was isolated as an orange solid in 31% yield. The presence of a hydride ligand in the complex is strongly supported by the ^{1}H NMR spectra of the orange solid, in dichloromethane-d_2, at room temperature, which contains a singlet at -25.62 ppm. In the ^{13}C{^{1}H} NMR spectrum, the resonance due the coordinated carbon atom of dpyMeb appears at 188.5 ppm. In agreement with the proven ability of hydrides of platinum group metal complexes to promote the intramolecular activation of C(sp^2)-H bonds,[23] complex **8** releases molecular hydrogen to afford the target compound Ir{κ^3-*C*,*N*,*N*-(IndpyC_6H_4)}{κ^3-*N*,*C*,*N*-(dpyMeb)} (**9**), as a result of the hydride-mediated *ortho*-CH bond activation of the aryl group of the κ^2-*N*,*N*-(indpyC_6H_5) ligand. Complex **9** was isolated as an orange solid in 30% yield, after the purification of the reaction crude by column chromatography.

Scheme 6. Preparation of Emitter 9

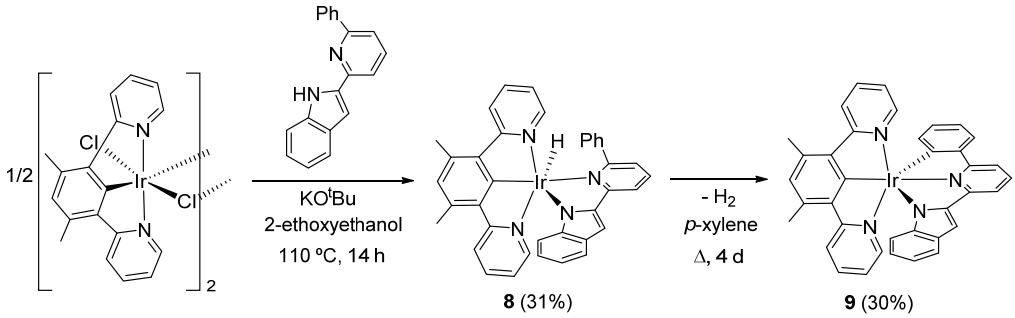

Complex **9** was characterized by X-ray diffraction analysis. Figure 5 gives a view of the molecule, which confirms the formation of the desired structure. The coordination polyhedron around the metal center resembles the distorted octahedrons of **6** and **7**. In this case, the angles between the donor atoms disposed mutually *trans* are 160.70(19)º (N(3)-Ir-N(4)), 175.3(2)º (C(32)-Ir-N(1)), and 155.5(2)º (C(1)-Ir-N(2)). The Ir-aryl$_{5t}$ and Ir-aryl$_{4t'}$ bond lengths of 1.933(6) Å (Ir-C(32)) and 2.031(6) (Ir-C(1)) Å, respectively, compare well with those of **6** and **7**. In the $^{13}C\{^1H\}$ NMR spectrum, the resonances corresponding to the metalated carbon atoms appears at 190.4 (5t) and 147.8 (4t') ppm, in agreement with those of **4**–**7**.

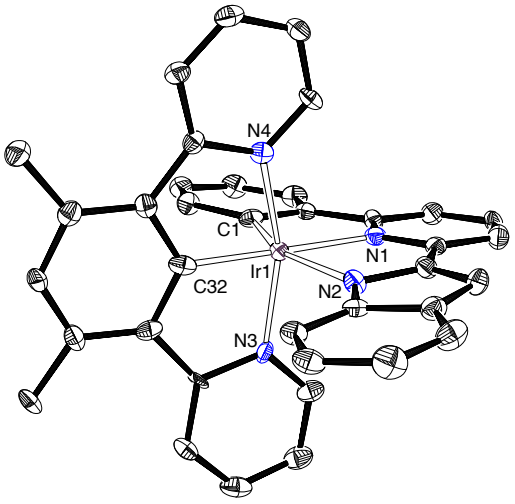

Figure 5. Molecular diagram of complex **9** (50% probability ellipsoids). Hydrogen atoms are omitted for clarity. Selected bond lengths (Å) and angles (deg): Ir-C(1) = 2.031(6), Ir-N(1) =

2.078(5), Ir-N(2) = 2.122(5), Ir-N(4) = 2.037(5), Ir-C(32) = 1.933(6), Ir-N(3) = 2.038(5), Ir-N(4) = 2.037(5); C(1)-Ir-N(2) = 155.5(2), N(3)-Ir-N(4) = 160.70(19), N(1)-Ir-C(32) = 175.3(2).

Photophysical and Electrochemical Properties of the [5t + 4t'] Emitters. Selected UV-vis absorption data for 2-methyltetrahydrofuran (MeTHF) solutions of **4**–**7** and **9** are collected in Table 1. In agreement with other emitters of this class,[10-13,15] three different regions are clearly observed in the spectra (Figures S1-S5): <300, 300–450 and >450 nm. According to time-dependent DFT calculations (B3LYP-GD3//SDD(f)6-31G**), which were performed in tetrahydrofuran as solvent, the absorptions of the highest energy can be assigned to $^{1}\pi$-π^* intra- and interligand transitions, whereas those situated in the intermediated zone are due to spin-allowed charge transfers from the metal to the 5t-ligand (MLCT) mixed with 4t'-to-5t (LLCT) and 5t-to-5t (ILCT) transitions (Tables S1-S10). The very weak absorptions tails after 450 nm correspond to formally spin-forbidden ^{3}MLCT transitions, which are produced by the large spin-orbit coupling introduced by the iridium center with some contribution from the $^{3}\pi$-π^* transitions.

Table 1. Selected Experimental UV-Vis Absorptions for 4–7 and 9 (in MeTHF) and Computed TD-DFT (in THF) Vertical Excitation Energies and their Major Contributions

λ_{exp} (nm)	ε (10^{-3} $M^{-1}\cdot cm^{-1}$)	excitation energy (nm)	oscillator strength, *f*	transition	character of the transition
			Complex **4**		
276	40.0	276	0.1754	HOMO-6 → LUMO (74%)	LLCT/ILCT (5t + 4t' →5t)
308	26.2	307	0.1206	HOMO-3 → LUMO+2 (70%)	MLCT/LLCT (Ir + 5t → 4t')
418	12.3	422	0.1015	HOMO-1 → LUMO (82%)	MLCT/LLCT/ILCT (Ir + 5t + 4t' → 5t)
		424 (S_1)	0.0154	HOMO → LUMO (96%)	MLCT/LLCT (Ir + 4t' → 5t)
500	2.6	482 (T_1)	0	HOMO-1→ LUMO (96%)	^{3}MLCT/^{3}LLCT/^{3}ILCT (Ir + 5t + 4t' → 5t)
			Complex **5**		
292	21.9	293	0.0793	HOMO-5 → LUMO (78%)	LLCT/ILCT (5t + 4t' →5t)
352	20.5	348	0.2403	HOMO-2 → LUMO+1 (86%)	MLCT/ILCT (Ir + 4t' → 4t')
400	11.8	397	0.1464	HOMO → LUMO+2 (78%)	MLCT/LLCT (Ir + 4t' → 5t)
418	11.6	421	0.0801	HOMO-1→ LUMO (72%)	MLCT/LLCT (Ir + 4t' → 5t)
		424 (S_1)	0.023	HOMO → LUMO (84%)	MLCT/LLCT (Ir + 4t' → 5t)
494		481 (T_1)	0	HOMO-1→ LUMO (95%)	^{3}MLCT/^{3}LLCT/^{3}ILCT (Ir + 5t + 4t' → 5t)
			Complex **6**		
262	37.6	269	0.2803	HOMO-5 → LUMO+2 (52%)	ILCT (4t' → 4t')
				HOMO-4 → LUMO+3 (25%)	LLCT (5t → 4t')
298	24.9	300	0.1431	HOMO-4→ LUMO (73%)	LLCT/ILCT (5t + 4t' →5t)
396	8.4	396	0.1276	HOMO→ LUMO+1 (77%)	MLCT/LLCT (Ir + 4t' → 5t)
420	8.4	414	0.0267	HOMO → LUMO (91%)	MLCT/LLCT (Ir + 4t' → 5t)
		418 (S_1)	0.0977	HOMO-1→ LUMO (79%)	MLCT/LLCT/ILCT (Ir + 5t + 4t' → 5t)
494	1.8	473 (T_1)	0	HOMO-1→ LUMO (95%)	^{3}MLCT/^{3}LLCT/^{3}ILCT (Ir + 5t + 4t' → 5t)
			Complex **7**		
272	22.4	273	0.1135	HOMO-6 → LUMO+1 (75%)	LLCT/ILCT (5t + 4t' →5t)
298	16.1	300	0.1085	HOMO-5 → LUMO+2 (82%)	LLCT/ILCT (5t + 4t' → 5t)
396	6.7	395	0.1568	HOMO → LUMO+2 (73%)	MLCT/LLCT (Ir + 4t' → 5t)
432	5.9	418 (S_1)	0.0848	HOMO-1→ LUMO (79%)	MLCT/LLCT/ILCT (Ir + 5t + 4t' → 5t)
492	1.3	472 (T_1)	0	HOMO-1→ LUMO (95%)	^{3}MLCT/^{3}LLCT/^{3}ILCT (Ir + 5t + 4t' → 5t)
			Complex **9**		
272	46.1	272	0.1016	HOMO-6 → LUMO+1 (60%)	LLCT (4t' → 5t)
				HOMO-3 → LUMO+5 (15%)	LLCT (4t' → 5t)
304	31.4	307	0.2163	HOMO-4 → LUMO+2 (74%)	MLCT/LLCT/ILCT (Ir + 5t + 4t' → 4t')
410	19.1	416	0.2004	HOMO-1→ LUMO (79%)	MLCT/LLCT/ILCT (Ir + 5t + 4t' → 5t)
472	6.2	456 (S_1)	0.0072	HOMO → LUMO (98%)	MLCT/LLCT (Ir + 4t' → 5t)
516	1.0	530 (T_1)	0	HOMO → LUMO + 2 (39%)	^{3}MLCT/^{3}ILCT (Ir + 4t' → 5t)
				HOMO → LUMO + 3 (40%)	^{3}MLCT/^{3}ILCT (Ir + 4t' → 5t)

The electrochemical behavior of the *bis*(tridentate) complexes was evaluated by cyclic voltammetry in dichloromethane (**4**–**7**) or acetonitrile (**9**) solutions under argon. The results are given in Table 2 and Figure S6. The HOMO and LUMO energy levels estimated from their oxidation potentials and emission spectra, respectively, along with DFT-calculated values are also included (Tables S11–S15 and Figures S7-S12). All complexes exhibit oxidation waves; however, reduction waves are not seen within the solvents electrochemical window. Compounds **4**–**7** show an irreversible oxidation process between 0.41 and 0.52 V vs Fc/Fc^+, whereas the indole derivative **9** exhibits an oxidation peak at 0.15 V vs Fc/Fc^+.[24] The HOMO energy levels determined from the oxidation potentials matches with those obtained from DFT calculations. The lower oxidation potential of **9** is consistent with its higher HOMO energy level with regard to those of **4**–**7**. Likewise, the LUMO energy levels obtained from the onsets of the emission spectra[12a,16d,25] show the same tendency that those found from DFT calculations.

Table 2. Electrochemical and DFT MO Energy Data for Complexes 4–7 and 9

		obs (eV)			calcd (eV)		
complex	E_{pa}^{ox} [a] (V)	HOMO[b]	E_{00}[c]	LUMO[d]	HOMO[e]	LUMO[e]	HLG[e,f]
4	0.45	-5.25	2.57	-2.68	-5.08	-1.59	3.49
5	0.52	-5.32	2.56	-2.76	-5.14	-1.60	3.54
6	0.41	-5.21	2.53	-2.68	-5.06	-1.49	3.57
7	0.47	-5.27	2.53	-2.74	-5.11	-1.50	3.61
9	0.15	-4.95	2.33	-2.62	-4.76	-1.46	3.30

[a]Measured in degassed dichloromethane (**4**–**7**) or acetonitrile solutions (**9**) vs Fc/Fc^+. [b]HOMO = $-[E^{ox}$ vs $Fc/Fc^+ + 4.8]$ eV. [c]E_{00} = onset of emission in MeTHF at 77 K. [d]LUMO = HOMO + E_{00}. [e]Values from electronic structure DFT calculations. [f]HLG = LUMO – HOMO.

Complexes **4–7** and **9** are phosphorescent emitters upon photoexcitation, in a doped poly(methyl methacrylate) (PMMA) film at 5 wt % at room temperature and in MeTHF at room temperature and at 77 K. The emission spectra are shown in Figure 6 and Figures S13–S27, whereas Table 3 summarizes calculated and experimental wavelengths, observed lifetimes, quantum yields, and radiative and nonradiative rate constants.

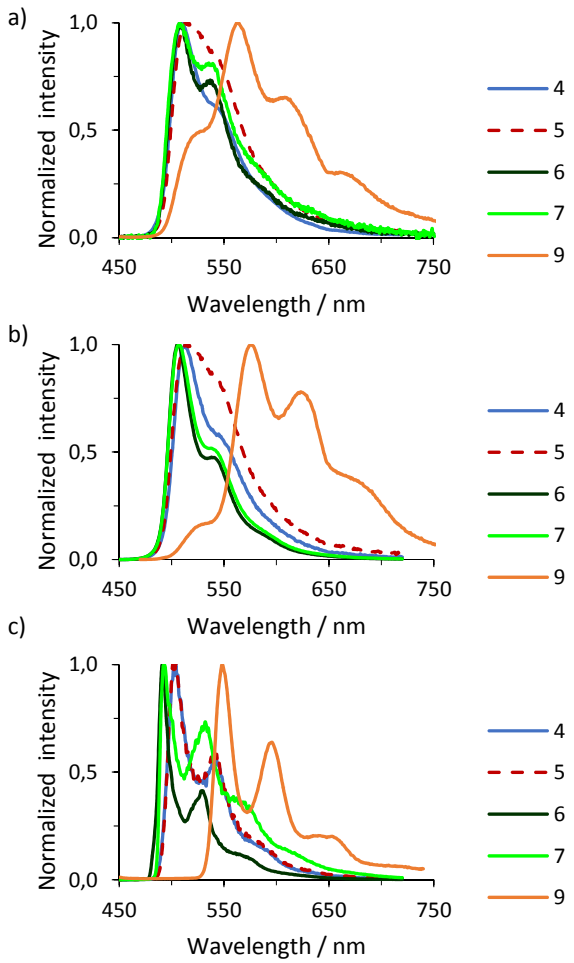

Figure 6. Emission spectra of complexes **4–7** and **9** recorded in 5 wt % PMMA films at 298 K (a), in MeTHF at 298 K (b), and in MeTHF at 77 K (c).

Table 3. Photophysical Data for Complexes 4–7 and 9

calc λ_{em} (nm)	media (T, K)	λ_{em} (nm)	λ_{exc} (nm)	τ (μs)	ϕ	$k_r{}^a$ (s^{-1})	$k_{nr}{}^a$ (s^{-1})	k_r/k_{nr}
			Complex **4**					
	PMMA (298)	510 (max), 541	429	1.2	0.37	3.1×10^5	5.3×10^5	0.6
537[b]	MeTHF (298)	512 (max), 547	434	0.8	0.35	4.4×10^5	8.1×10^5	0.5
	MeTHF (77)	503 (max), 542	428	9.7				
			Complex **5**					
	PMMA (298)	514 (max), 541	430	0.5	0.40	8.0×10^5	1.2×10^6	0.7
535[b]	MeTHF (298)	514 (max), 547	432	0.6	0.37	6.2×10^5	1.1×10^6	0.6
	MeTHF (77)	502 (max), 540	427	8.8				
			Complex **6**					
	PMMA (298)	509 (max), 534	439	2.5	0.61	2.4×10^5	1.6×10^5	1.6
517[b]	MeTHF (298)	506 (max), 540	306	1.4	0.64	4.6×10^5	2.6×10^5	1.8
	MeTHF (77)	491 (max), 529	318	2.5				
			Complex **7**					
	PMMA (298)	508 (max), 535	429	2.1	0.68	3.2×10^5	1.5×10^5	2.1
520[b]	MeTHF (298)	507 (max), 538	300	1.5	0.52	3.5×10^5	3.2×10^5	1.1
	MeTHF (77)	493 (max), 532	310	3.6				
			Complex **9**					
	PMMA (298)	564 (max), 609	379	2.5	0.30	1.2×10^5	2.8×10^5	0.4
559[c]	MeTHF (298)	576 (max), 624	383	1.3	0.20	1.5×10^5	6.2×10^5	0.3
	MeTHF (77)	547 (max), 594	377	3.0				

[a]Calculated according to the equations $k_r = \phi/\tau$ and $k_{nr} = (1 - \phi)/\tau$, where k_r is the radiative rate constant, k_{nr} is the nonradiative rate constant, ϕ is the quantum yield, and τ is the excited-state lifetime. [b]Predicted from TD-DFT calculations in THF at 298 K by estimating the energy difference between the optimized T_1 and singlet state S_0. [c]Predicted from TD-DFT calculations in THF at 298 K by estimating the energy difference between the optimized T_1 and singlet state with the same geometry.

Complexes **4**–**7** are emissive in the green spectral region (490–550 nm). The presence of methyl groups at positions 3 and 5 of the phenyl linker of the 5t ligand or the replacement of the imidazole moiety by benzimidazole in the 4t' group does not influence on the emission color. Thus, the spectra of the four compounds are almost identical, which is consistent with similar HOMO-LUMO gaps (3.49–3.61 eV). All the emission spectra display vibronic structures in

agreement with a notable contribution of ligand-centered $^3\pi$-π^* transitions to the excited states.[12a,13,15a-b,16c] Because the emissions can be attributed to T_1 excited states, there is also good agreement between the experimental wavelengths and those calculated by estimating the difference in energy between the optimized triplet states T_1 and the singlet states S_0 in tetrahydrofuran. On the other hand, complex **9** is greenish yellow emissive with maximums between 547 and 624 nm. The replacement of the benzimidazole moiety of **7** by indole produces a destabilization of the HOMO, which is now mainly centered on the indole group (Figure S11). As a result of the destabilization, a reduction of the HOMO-LUMO gap (3.30 eV) takes place, which gives rise to the shift of the emission towards lower energy. For the five complexes the observed lifetimes are short, lying in the range 0.5–9.7 μs. In contrast to the emission color, the quantum yield is sensitive to the methyl groups of the dpyMeb ligand but not to the change of imidazole by benzimidazole in the 4t' pincer. The presence of the methyl groups in the linker of the 5t ligand increases the efficiency of the emitters. While for **6** and **7** the quantum yields lie in the range 0.5–0.7, those of **4** and **5** are about 0.4. A similar effect has been observed in heteroleptic iridium(III) emitters bearing three 3e-donor bidentate ligands, two orthometalated phenyl-pyridines and an acetylacetonate.[26] The replacement of the benzimidazole moiety of **7** by indole produces a reddish displacement of the emission and a reduction of the efficiency of the emitter. Complexes with lower quantum yield; **4**, **5**, and **9**; display nonradiative rate constants which are one order of magnitude higher than the radiative rate constants, whereas both rate constants are of the same order of magnitude for **6** and **7**. The *bis*-NHC counterparts of complexes **4**–**7** depicted in Scheme 2 display emissions between 482 and 590 nm with quantum yields in PMMA film and in MeTHF solution between 0.73 and 0.49.[13]

Concluding Remarks

This study shows the preparation and photophysical properties of new molecular emitters [5t + 4t'] of iridium(III) including the 5t ligand resulting from the deprotonation at position 2 of the aryl group of 1,3-di(2-pyridyl)benzene (dpyb). In spite of that the coordination of dpyb to iridium(III) as a pincer has been challenged, we reveal that the treatment of the iridium(I) dimer $[Ir(\mu\text{-}Cl)(\eta^2\text{-}COE)_2]_2$ with Hg(dpyb)Cl produces a mercury-to-iridium transfer of the dpyb and chloride ligands to afford the iridium(III) derivative $IrCl_2\{\kappa^3\text{-}N,C,N\text{-}(dpyb)\}(\eta^2\text{-}COE)$, which is a useful starting point to prepare this class of emitters with dpyb as 5t ligand. As a proof of concept, we show that the reactions of this compound with 2-(1*H*-imidazol-2-yl)-6-phenylpyridine ($HNImpyC_6H_5$) and 2-(1*H*-benzimidazol-2-yl)-6-phenylpyridine ($HNBzimpyC_6H_5$) in the presence of Na_2CO_3 lead to the complexes $Ir\{\kappa^3\text{-}C,N,N\text{-}(NImpyC_6H_4)\}\{\kappa^3\text{-}N,C,N\text{-}(dpyb)\}$ and $Ir\{\kappa^3\text{-}C,N,N\text{-}(NBzimpyC_6H_4)\}\{\kappa^3\text{-}N,C,N\text{-}(dpyb)\}$, respectively, which are emissive in the green spectral region with quantum yields of about 0.4. The efficiency of these emitters is improved without affecting their color emissions, when methyl substituents are incorporated at positions 3 and 5 of the benzene ring of the dpyb ligand. The resulting green emitters $Ir\{\kappa^3\text{-}C,N,N\text{-}(NImpyC_6H_4)\}\{\kappa^3\text{-}N,C,N\text{-}(dpyMeb)\}$ and $Ir\{\kappa^3\text{-}C,N,N\text{-}(NBzimpyC_6H_4)\}\{\kappa^3\text{-}N,C,N\text{-}(dpyMeb)\}$ increase significantly their quantum yield until 0.5–0.7. The emissive properties of these complexes can be also modified by addressing the azole group of the 4t' ligand. For instance, the replacement of the benzimidazole group of $Ir\{\kappa^3\text{-}C,N,N\text{-}(NBzimpyC_6H_4)\}\{\kappa^3\text{-}N,C,N\text{-}(dpyMeb)\}$ by indole gives rise to a reddish displacement of the emission and the reduction of the quantum yield until 0.2–0.3.

In summary, this paper points out the way to prepare molecular emitters [5t+4t'] of iridium(III) with a 5t ligand resulting from the deprotonation at position 2 of the aryl group of 1,3-di(2-

pyridyl)benzene and compares their photophysical properties with those of the emitters resulting from the deprotonation of the dimethylated molecule 1,3-di(2-pyridyl)-4,6-dimethylbenzene at the same position.

Experimental Section

General Information. All reactions were run under inert atmosphere (argon) using Schlenk-tube techniques. [Ir(μ-Cl)(η^2-COE)$_2$]$_2$,[27] [IrCl(μ-Cl){κ^3-*N*,*C*,*N*-(dpyMeb)}]$_2$,[10,11] Hg(dpyb)Cl,[20,28] 2-(1*H*-imidazol-2-yl)-6-phenylpyridine,[29] 2-(1*H*-benzimidazol-2-yl)-6-phenylpyridine,[30] and 2-(6-phenylpyridine-2-yl)-1*H*-indole[31] were prepared according to the published procedures. In the NMR spectra (Figures S28–S45), chemical shifts (expressed in parts per million) are referenced to residual solvent peaks and coupling constants (*J*) are given in hertz (Hz).

Preparation of [IrCl(μ-Cl){κ^3-*N*,*C*,*N*-(dpyb)}]$_2$ (1). $IrCl_3 \cdot 3H_2O$ (150 mg, 0.411 mmol) and Hg(dpyb)Cl (231 mg, 0.493 mmol) were heated in 2-ethoxyethanol/water (12 mL/4 mL) at 80 ºC for 24 h. The orange solid formed was collected and washed with water (3 x 15 mL), ethanol (3 x 15 mL) and diethyl ether (3 x 15 mL). Yield: 143 mg (70%). Anal. Calcd. for $C_{32}H_{22}Cl_4Ir_2N_4$: C, 38.87; H, 2.24; N, 5.67. Found: C, 38.91; H, 2.08; N, 5.20.

Preparation of IrCl$_2${κ^3-*N*,*C*,*N*-(dpyb)}{κ-*S*-(DMSO)} (2). A suspension of **1** (75 mg, 0.076 mmol) was heated in 6 mL of DMSO at 80 ºC. The orange suspension changed to a yellow solution. This solution was filtrated through Celite and evaporated to dryness. The crude was washed with toluene (3 x 5 mL) and acetone (until the liquors were clear) to give a yellow solid. Yield: 20 mg (23%). Anal. Calcd. for $C_{18}H_{17}Cl_2IrN_2OS$: C, 37.76; H, 2.99; N, 4.89; S, 5.60. Found: C, 37.65; H, 3.29; N, 4.99; S, 5.97. MALDI (*m*/*z*): calcd for $C_{18}H_{17}ClIrN_2OS$ $[M\text{-}Cl]^+$ 537.0; found: 537.0. IR (cm^{-1}): ν(S=O) 1011 (s). ^{1}H NMR (300 MHz, DMSO-d_6, 298 K): δ 9.03 (d, $^3J_{H\text{-}H}$ = 5.3, 2H, NCH), 8.29 (d, $^3J_{H\text{-}H}$ = 7.9, 2H, py), 8.10 (m, 2H, py), 7.98 (d, $^3J_{H\text{-}H}$ = 7.6, 2H,

C_6H_3), 7.57 (m, 2H, py), 7.32 (t, $^3J_{H\text{-}H}$ = 7.6, 1H, C_6H_3), 2.73 (s, 6H, DMSO). $^{13}C\{^1H\}$-APT NMR (75 MHz, DMSO-d_6, 298 K): δ 167.2 ($2NC_q$), 165.2 (IrC), 152.7 (2NCH), 140.7 ($2C_q$ C_6H_3), 139.8 (2CH py), 125.5 (2CH C_6H_3), 124.0 (2CH py), 123.1 (CH C_6H_3), 120.7 (2CH py), 41.0 (DMSO).

Preparation of $IrCl_2\{\kappa^3$-*N*,*C*,*N*-(dpyb)$\}(\eta^2$-COE) (3). [Ir(μ-Cl)(η^2-COE)$_2$]$_2$ (300 mg, 0.335 mmol) and Hg(dpyb)Cl (313 mg, 0.670 mmol) in 25 mL of THF were stirred for 4 h. Then, the mixture was evaporated to dryness and extracted with dichloromethane (3 x 7 mL). After that, the solvent was evaporated and the residue was washed with propan-2-ol (4 x 7 mL) and diethyl ether (3 x 3 mL) to obtain a yellow solid. Yield: 207 mg (51%). Anal. Calcd. for $C_{24}H_{25}Cl_2IrN_2$: C, 47.68; H, 4.17; N, 4.63. Found: C, 47.25; H, 3.92; N, 4.81. HRMS (ESI+, *m*/*z*): calcd for $C_{24}H_{25}ClIrN_2$ $[M\text{-}Cl]^+$ 569.1336; found: 569.1288. ^1H NMR (400 MHz, CD_2Cl_2, 298 K): δ 9.23 (dt, $^3J_{H\text{-}H}$ = 5.8, $^4J_{H\text{-}H}$ = 1.5, 2H, NCH), 7.96–7.86 (m, 4H, py), 7.73 (d, $^3J_{H\text{-}H}$ = 7.7, 2H, C_6H_3), 7.39 (ddd, $^3J_{H\text{-}H}$ = 7.4, $^3J_{H\text{-}H}$ = 5.8, $^4J_{H\text{-}H}$ = 1.5, 2H, py), 7.25 (t, $^3J_{H\text{-}H}$ = 7.7, 1H, C_6H_3), 4.47–4.37 (m, 2H, CH COE), 1.57–1.44, 1.35–1.18 (both m, 3H each, CH_2 COE), 1.13–1.01, 0.99–0.83, 0.72–0.61 (all m, 2H each, CH_2 COE). $^{13}C\{^1H\}$-APT NMR ~~plus HSQC and HMBC~~ (100 MHz, CD_2Cl_2, 298 K): 167.5 ($2NC_q$), 166.9 (IrC, C_6H_3), 153.7 (2NCH), 141.3 ($2C_q$ C_6H_3), 139.3 (2CH py), 125.6 (2CH C_6H_3), 124.4 (2CH py), 123.4 (CH C_6H_3), 120.9 (2CH py), 89.8 (2CH= COE), 30.0, 26.7, 24.9 ($2CH_2$ each, COE).

Preparation of Ir$\{\kappa^3$-*C*,*N*,*N*-(NImpyC_6H_4)$\}\{\kappa^3$-*N*,*C*,*N*-(dpyb)$\}$ (4). Complex **3** (150 mg, 0.248 mmol), 2-(1*H*-imidazol-2-yl)-6-phenylpyridine (54.8 mg, 0.248 mmol), and sodium carbonate (131.4 mg, 1.240 mmol) were suspended in 10 mL of 2-ethoxyethanol and the suspension was heated at 135 ºC for 3 d. Then, the mixture was dried under vacuum and the crude was extracted with dichloromethane (3 x 7 mL). This orange solution was evaporated to

dryness and the addition of 5 mL of methanol caused the precipitation of a yellow solid, which was washed with MeOH (2 x 2 mL) and diethyl ether (2 x 2 mL). A yellow solid was obtained after column chromatography purification (SiO_2; 230–400 mesh), using a CH_2Cl_2/MeOH mixture (100:2 to 100:10) as eluent. Yield: 38 mg (24%). Anal. Calcd. for $C_{30}H_{20}IrN_5$: C, 56.06; H, 3.14; N, 10.90. Found: C, 55.70; H, 3.19; N, 10.57. HRMS (ESI+, *m*/*z*): calcd for $C_{30}H_{21}IrN_5$ $[M+H]^+$ 644.1422; found: 644.1437. T_d = 390 ºC (Figure S46).[32] ^{1}H NMR (300 MHz, CD_2Cl_2, 298 K): δ 8.16 (d, $^3J_{H\text{-}H}$ = 7.7, 1H, *py*-Im), 8.01–7.87 (m, 5H, 2H C_6H_3 + 2H py dpyb + 1H *py*-Im), 7.80 (d, $^3J_{H\text{-}H}$ = 7.7, 1H, *py*-Im), 7.66–7.52 (m, 3H, 2H py dpyb + 1H C_6H_4), 7.49–7.38 (m, 3H, 2CHN py + 1H C_6H_3), 6.88 (s, 1H, Im), 6.81–6.66 (m, 3H, 2H py dpyb + 1H C_6H_4), 6.51 (dd, $^3J_{H\text{-}H}$ = $^3J_{H\text{-}H}$ = 7.5, 1H, C_6H_4), 6.11 (s, 1H, Im), 5.79 (d, $^3J_{H\text{-}H}$ = 7.5, 1H, 1H C_6H_4). $^{13}C\{^1H\}$-APT NMR (75 MHz, CD_2Cl_2, 298 K): δ 185.5 (IrC C_6H_3), 169.8 (2NC_q, py dpyb), 163.1 (NC_q, *py*-Im), 155.5 (NCN), 151.8 (NC_q, *py*-C_6H_4), 151.2 (2NCH py), 147.7 (IrC, C_6H_4), 147.0 (C_q, *C_6H_4*-py), 140.6 (2C_q C_6H_3), 139.2 (CH *py*-Im), 136.8 (2CH, py dpyb), 136.7 (CH, C_6H_4), 130.1 (CH, Im), 129.6 (CH, C_6H_4), 128.5 (CH, Im), 125.1 (2CH, C_6H_3), 125.1 (CH, C_6H_4), 122.7 (2CH, py dpyb), 122.4 (CH, C_6H_4), 120.2 (CH, C_6H_3), 119.9 (2CH, py dpyb), 116.0, 114.8 (both CH, *py*-Im).

Preparation of Ir{*κ*^{3}-*C*,*N*,*N*-(NBzimpyC_6H_4){*κ*^{3}-*N*,*C*,*N*-(dpyb)} (5). This complex was prepared similarly to compound **4**, starting from **3** (150 mg, 0.248 mmol), 2-(1*H*-benzimidazol-2-yl)-6-phenylpyridine (67.2 mg, 0.248 mmol), and sodium carbonate (131.4 mg, 1.240 mmol) and heating for 36 h. A yellow solid was obtained after column chromatography purification (SiO_2; 230–400 mesh), using a CH_2Cl_2/MeOH mixture (100:1 to 100:5) as eluent. Yield: 23 mg (14%). Anal. Calcd. for $C_{34}H_{22}IrN_5$: C, 58.95; H, 3.20; N, 10.11. Found: C, 58.60; H, 3.27; N, 10.42. HRMS (ESI+, *m*/*z*): calcd for $C_{34}H_{23}IrN_5$ $[M+H]^+$ 694.1579; found: 694.1573. T_d = 402 ºC (Figure S46).[32] ^{1}H NMR (300 MHz, CD_2Cl_2, 298 K): δ 8.35 (d, $^3J_{H\text{-}H}$ = 7.6, 1H, *py*-Bzim), 8.14–

8.02 (m, 3H, 2H C_6H_3 + 1H *py*-Bzim), 8.02–7.90 (m, 3H, 2H py dpyb + 1H *py*-Bzim), 7.70 (d, $^3J_{H\text{-}H}$ = 7.8, 1H, C_6H_4), 7.62–7.50 (m, 3H, 1H C_6H_3 + 2H py dpyb), 7.49–7.38 (m, 3H, 2NCH + 1H Bzim), 6.87–6.77 (m, 2H, 1H C_6H_4 + 1H Bzim), 6.72 (dd, $^3J_{H\text{-}H}$ = $^3J_{H\text{-}H}$ = 6.6, 2H, py dpyb), 6,56 (m, 2H, 1H C_6H_4 + 1H Bzim), 5.98 (d, $^3J_{H\text{-}H}$ = 7.8, 1H, Bzim), 5.94 (d, $^3J_{H\text{-}H}$ = 7.8, 1H, C_6H_4). $^{13}C\{^1H\}$-APT NMR (75 MHz, CD_2Cl_2, 298 K): δ 185.2 (IrC, C_6H_3), 169.9 (2NC_q, dpyb), 163.7 (NC_q, *py*-Bzim), 162.2 (NCN), 152.6 (NC_q, *py*-C_6H_4), 151.1 (2NCH), 149.1 (C_q, C_6H_4), 146.7 (IrC C_6H_4), 145.8, 145.0 (both C_q, Bzim), 140.6 (2C_q C_6H_3), 139.2 (CH, *py*-Bzim), 136.8 (3CH, 2CH py dpyb + 1CH C_6H_4), 129.8, 125.4 (both CH, C_6H_4), 125.2 (2CH, C_6H_3), 122.7 (2CH, py dpyb), 122.4 (CH C_6H_4), 121.6 (CH, Bzim), 120.4 (CH C_6H_3), 120.3 (CH, Bzim), 119.9 (2CH, py dpyb), 119.3 (CH, Bzim), 118.0, 116.9 (both CH, *py*-Bzim), 114.5 (CH, Bzim).

Preparation of Ir{κ^3-*C*,*N*,*N*-(NImpyC_6H_4){κ^3-*N*,*C*,*N*-(dpyMeb)} (6). [IrCl(μ-Cl){κ^3-*N*,*C*,*N*-(dpyMeb)}]$_2$ (400 mg, 0.382 mmol), 2-(1*H*-imidazol-2-yl)-6-phenylpyridine (169.3 mg, 0.766 mmol), and sodium carbonate (202.8 mg, 1.913 mmol) in 2-ethoxyethanol (35 mL) were heated at 135 ºC, for 3d. After cooling to room temperature, the mixture was dried under vacuum and the resulting orange solid was extracted with dichloromethane (3 x 4 mL). Then the solution was concentrated and addition of methanol caused the precipitation of a yellow solid which was washed with MeOH (4 x 10 mL), a CH_2Cl_2/Et_2O mixture (1:4) (3 x 12 mL), and Et_2O (3 x 10 mL) and dried under vacuum at 100 ºC for 3 days. Yield: 281 mg (55%). Anal. Calcd for $C_{32}H_{24}IrN_5 \cdot H_2O$: C, 55.80; H, 3.80; N, 10.17. Found: C, 55.96; H, 3.84; N, 10.11. HRMS (electrospray, *m*/*z*): calcd for $C_{32}H_{25}IrN_5$ $[M+H]^+$ 672.1739; found 672.1735. T_d = 415 ºC (Figures S46-S47).[32] ^1H NMR (400 MHz, CD_2Cl_2, 298 K): δ 8.08 (d, $^3J_{H\text{-}H}$ = 8.4, 2H, py dpyMeb), 7.96 (d, $^3J_{H\text{-}H}$ = 7.5, 1H, *py*-Im), 7.90 (dd, $^3J_{H\text{-}H}$ = $^3J_{H\text{-}H}$ = 7.5, 1H, *py*-Im), 7.75 (d, $^3J_{H\text{-}H}$ = 7.5, 1H, *py*-Im), 7.62–7.55 (m, 3H, 2H py dpyMeb + 1H C_6H_4), 7.50 (d, $^3J_{H\text{-}H}$ = 5.6, 2H, NCH py), 7.04 (s, 1H,

dpyMe*b*), 6.84 (s, 1H, Im), 6.77–6.71 (m, 3H, 1H C_6H_4 + 2H py dpyMeb), 6.51 (ddd, $^3J_{H\text{-}H}$ = $^3J_{H\text{-}H}$ = 7.5, $^4J_{H\text{-}H}$ = 1.4, 1H, C_6H_4), 6.08 (s, 1H, Im), 5.83 (dd, 1H, $^3J_{H\text{-}H}$ = 7.5, $^4J_{H\text{-}H}$ = 0.9, 1H, C_6H_4), 2.92 (s, 6H, Me). $^{13}C\{^1H\}$-APT NMR (100 MHz, CD_2Cl_2, 298 K): δ 189.5 (IrC, dpyMe*b*), 170.6 ($2NC_q$, py dpyMeb), 162.9 (NC_q, *py*-Im), 156.1 (NCN), 152.6 (NC_q, *py*-C_6H_4), 150.8 (2NCH, py), 149.3 (C_q, *C_6H_4*-py), 147.1 (IrC, C_6H_4), 138.9 (CH, *py*-Im), 137.8 ($2C_q$, dpyMe*b*), 137.1 (CH, C_6H_4), 136.9 ($2C_q$-Me), 136.1 (2CH, py dpyMeb), 130.2 (2CH, Im), 129.4 (CH, C_6H_4), 128.6 (CH, dpyMe*b*), 125.0 (CH, C_6H_4), 123.0 (2CH, py dpyMeb), 122.2 (CH, C_6H_4), 121.7 (2CH, py dpyMeb), 115.3, 114.2 (both CH, *py*-Im), 23.0 (2Me).

Preparation of Ir{κ^3-*C*,*N*,*N*-(NBzimpyC_6H_4){κ^3-*N*,*C*,*N*-(dpyMeb)} (7). This complex was prepared similarly to compound **6**, but heating for 24 h, starting from [IrCl(μ-Cl){κ^3-*N*,*C*,*N*-(dpyMeb)}]$_2$ (400 mg, 0.382 mmol), 2-(1*H*-benzimidazol-2-yl)-6-phenylpyridine (207.6 mg, 0.766 mmol), and sodium carbonate (202.8 mg, 1.913 mmol). Yellow solid. Yield: 318 mg (58%). Anal. Calcd for $C_{36}H_{26}IrN_5 \cdot H_2O$: C, 58.52; H, 3.82; N 9.48. Found: C 58.77, H 3.80, N, 9.38. HRMS (electrospray, *m*/*z*): calcd for $C_{36}H_{27}IrN_5$ $[M+H]^+$ 722.1896; found 722.1896. T_d = 444 ºC (Figure S46-S47).[32] ^1H NMR (400 MHz, CD_2Cl_2, 298 K): δ 8.31 (d, $^3J_{H\text{-}H}$ = 7.8, 1H, *py*-Bzim), 8.06 (d, $^3J_{H\text{-}H}$ = 8.4, 2H, 2H py dpyMeb), 8.04 (dd, $^3J_{H\text{-}H}$ = $^3J_{H\text{-}H}$ = 7.8, 1H, *py*-Bzim), 7.97 (d, $^3J_{H\text{-}H}$ = 7.8, 1H, *py*-Bzim), 7.69 (d, $^3J_{H\text{-}H}$ = 7.8, 1H, C_6H_4), 7.52–7.44 (m, 5H, 4H py dpyMeb + 1H Bzim), 7.14 (s, 1H, dpyMe*b*), 6.83–6.78 (m, 2H, 1H Bzim + 1H C_6H_4), 6.65 (dd, $^3J_{H\text{-}H}$ = $^3J_{H\text{-}H}$ = 6.6, 2H, py dpyMeb), 6.60-6.52 (m, 2H, 1H Bzim + 1H C_6H_4), 6.03 (d, $^3J_{H\text{-}H}$ = 8.0, 1H, C_6H_4), 5.96 (d, $^3J_{H\text{-}H}$ = 7.5, 1H, Bzim), 2.96 (s, 6H, Me). $^{13}C\{^1H\}$-APT NMR (100 MHz, CD_2Cl_2, 298 K): δ 188.8 (IrC, dpyMe*b*), 170.7 ($2NC_q$, py dpyMeb), 163.6 (NC_q, *py*-Bzim), 162.5 (NCN), 152.7 (NC_q, *py*-C_6H_4), 150.7 (2NCH), 150.2 (C_q, *C_6H_4*-py), 146.6 (C_q, Bzim), 146.1 (IrC, C_6H_4), 145.1 (C_q, Bzim), 139.1 (CH, *py*-Bzim), 137.9 ($2C_q$, dpyMe*b*), 137.0 (CH, Bzim), 137.0 (C_q-

Me), 136.2 (2CH, py dpyMeb), 129.8 (CH, Bzim), 128.8 (CH, dpyMe*b*), 125.4 (CH, C_6H_4), 123.0 (2CH, py dpyMeb), 122.3 (CH, C_6H_4), 121.7 (2CH, py dpyMeb), 121.4 (CH, C_6H_4), 120.2, 119.4 (both CH, Bzim), 117.9, 116.8 (both CH *py*-Bzim), 114.7 (CH, C_6H_4), 23.0 (2Me).

Preparation of IrH{κ^2-*N*,*N*-(IndpyC$_6$H$_5$){κ^3-*N*,*C*,*N*-(dpyMeb)} (8). [IrCl(μ-Cl){κ^3-*N*,*C*,*N*-(dpyMeb)}]$_2$ (150 mg, 0.143 mmol), 2-(6-phenylpyridin-2-yl)-1*H*-indole (77.5 mg, 0.287 mmol), and KO^{t}Bu (80.5 mg, 0.717 mmol) in 2-ethoxyethanol (15 mL) were heated at 110 ºC overnight. After cooling to room temperature and subsequent removal of the solvent, the resulting orange solid was extracted with toluene (4 x 4 mL). This solution was concentrated and addition of pentane caused the precipitation of an orange solid, which was washed with pentane (3 x 10 mL) and dried under vacuum. Yield: (64 mg, 31%). Anal. Calcd for $C_{37}H_{29}IrN_4$: C, 61.56; H, 4.05; N, 7.76. Found: C 61.30, H 4.32, N, 7.32. HRMS (electrospray, *m*/*z*): calcd for $C_{37}H_{30}IrN_4$ $[M+H]^+$ 723.2096; found 723.2107. ^{1}H NMR (400 MHz, CD_2Cl_2, 298 K): δ 8.05 (dd, $^3J_{H\text{-}H}$ = 7.8, $^4J_{H\text{-}H}$ = 1.4, 1H, *py*-Ind), 7.88 (d, $^3J_{H\text{-}H}$ = 8.3, 2H, py dpyMeb), 7.80 (m, 2H, py dpyMeb), 7.74 (m, 1H, Ind), 7.60 (m, 2H, py dpyMeb), 7.51 (dd, $^3J_{H\text{-}H}$ = $^3J_{H\text{-}H}$ = 7.8, 1H, py-Ind), 7.42 (m, 1H, Ind), 7.33 (d, $^4J_{H\text{-}H}$ = 1.0, 1H, Ind), 6.95, 6.90 (both m, 1H each, Ind), 6.88 (m, 1H, H^p Ph ppyindH), 6.72 (ddd, $^3J_{H\text{-}H}$ =7.2, $^3J_{H\text{-}H}$ = 5.7, $^4J_{H\text{-}H}$ = 1.0, 2H, H py dpyMeb), 6.65, (m, 2H, H^m Ph), 6.50 (s, 1H, dpyMe*b*), 6.44 (dd, $^3J_{H\text{-}H}$ = 7.8, $^4J_{H\text{-}H}$ = 1.4, 1H, *py*-Ind), 5.94 (dd, $^3J_{H\text{-}H}$ = 8.1, $^4J_{H\text{-}H}$ = 1.2, 2H, H^o Ph), 2.64 (s, 6H, Me), -25.62 (s, 1H, Ir-H). ^{13}C{^{1}H}-APT NMR (100 MHz, CD_2Cl_2, 298 K): δ 188.5 (IrC), 172.2 (NC$_q$, py dpyMeb), 163.6 (N*C*$_q$, *py*-Ph), 159.6 (N*C*$_q$, *py*-Ind), 152.4 (2NCH), 148.6, 148.1 (both NC$_q$, Ind), 136.5 (CH, *py*-Ind), 139.3 (C$_q$, ipso-Ph), 138.3 (2*C*$_q$-Me), 136.5 (CH, *py*-Ind), 136.2 (2*C*$_q$-py, dpyMe*b*), 135.4 (2CH, py dpyMeb), 131.5 (CH*C*$_q$CH, Ind), 127.7 (C^{p}H, Ph), 127.3 (2C^{o}H, Ph), 126.9 (CH, dpyMe*b*), 126.8 (2C^{m}H, Ph), 122.2 (2CH, py dpyMeb),

122.1 (CH, *py*-Ind), 121.1 (CH Ind), 121.0 (2CH, py dpyMeb), 120.6 (CH Ind), 119.4 (CH, *py*-Ind), 118.1, (2 CH, Ind), 101.2 (C_qCHC_q, Ind), 22.7 (2Me).

Preparation of Ir{κ^3-*C*,*N*,*N*-(IndpyC$_6$H$_4$){κ^3-*N*,*C*,*N*-(dpyMeb)} (9). Complex **8** (73 mg, 0.101 mmol) was heated in *p*-xylene under reflux for 4 days. After cooling to room temperature, *p*-xylene was removed under vacuum and the resulting brown-orange solid was purified on a column chromatography (SiO_2; 230–400 mesh) using a toluene/CH_2Cl_2 mixture (4:1) as eluent. An orange solid was obtained and it was washed with pentane (3 x 6 mL). Yield: 21.5 mg, 0.03 mmol, 30%). Anal. Calcd for $C_{37}H_{27}IrN_4$: C, 61.73; H, 3.78; N 7.78. Found: C 61.41, H 3.77, N, 7.42. HRMS (electrospray, *m*/*z*): calcd for $C_{37}H_{28}IrN_4$ $[M+H]^+$ 720.8624; found 720.8593. T_d = 424 ºC (Figure S46).[32] ^{1}H NMR (300 MHz, CD_2Cl_2, 298 K): 8.07 (d, $^3J_{H-H}$ = 8.5, 2H, py dpyMeb), 7.93 (m, 2H, *py*-Ind), 7.79 (m, 1H, *py*-Ind), 7.64 (d, $^3J_{H-H}$ = 7.5, 1H, C_6H_4), 7.54-7.47 (m, 4H, py dpyMeb), 7.29 (d, $^3J_{H-H}$ = 7.9, 1H, Ind), 7.15 (s, 1H, dpyMe*b*), 6.97 (s, 1H, Ind), 6.76 (dd, $^3J_{H-H}$ = $^3J_{H-H}$ = 7.5, 1H, C_6H_4), 6.65 (dd, $^3J_{H-H}$ = $^3J_{H-H}$ = 6.5, 2H, py dpyMeb), 6.54 (m, 2H, 1H C_6H_4 + 1H Ind), 6.35 (dd, $^3J_{H-H}$ = $^3J_{H-H}$ = 7.5, 1H, Ind), 5.88 (d, $^3J_{H-H}$ = 7.5, 1H, C_6H_4), 5.82 (d, $^3J_{H-H}$ = 7.5, 1H, Ind), 2.97 (s, 6H, Me). ^{13}C{^{1}H}-APT NMR (75 MHz, CD_2Cl_2, 298 K): 190.4 (IrC, dpyMeb), 170.7 ($2NC_q$, py dpyMeb), 162.7, 156.0 (both C_q, *py*-Ind), 151.2 (C_q, C_6H_4), 150.6 (2CH, py dpyMeb), 148.3 (NC_q, Ind), 147.8 (IrC_q, C_6H_4), 147.6 (C_q, Ind), 138.2 (CH, *py*-Ind), 137.8 ($2C_q$, dpyMe*b*), 137.0 (CH, C_6H_4), 136.9 ($2C_q$, dpyMe*b*), 135.8 (2CH, py dpyMeb), 129.9 (C_q, Ind), 129.3 (CH, Ind or C_6H_4), 128.4 (CH, dpyMe*b*), 125.2 (CH, C_6H_4), 122.8 (2CH, py dpyMeb), 121.9 (CH, C_6H_4), 121.5 (2CH, py dpyMeb), 121.3, 121.0 (both CH, Indol), 117.1 (CH, Ind or C_6H_4), 116.0 (CH, *py*-Ind), 115.0 (CH, Ind), 114.2 (CH, *py*-Ind), 102.6 (C_qCHC_q, Ind), 23.0 (2Me).

ASSOCIATED CONTENT

Supporting Information

The Supporting Information is available free of charge on the ACS publications web site.

General information for the experimental section; crystallographic data; computational details; cyclic voltammograms; experimental and computed UV/vis spectra; frontier molecular orbitals and natural transition orbitals; normalized excitation and emission spectra; NMR spectra; TGA and DSC curves (PDF)

Cartesian coordinates of the optimized structures (XYZ).

Accession codes

CCDC 1968295-1968299 contain the crystallographic data for this paper. These data can be obtained free of charge *via* www.ccdc.cam.ac.uk/data_request/cif, or by e-mailing data_request@ccdc.cam.ac.uk, or by contacting The Cambridge Crystallographic Data Centre, 12 Union Road, Cambridge CB2 1EZ, UK; fax: +44 1223 336033.

AUTHOR INFORMATION

Corresponding Author

* E-mail: maester@unizar.es.

Author Contributions

The manuscript was written through contributions of all authors. All authors have given approval to the final version of the manuscript.

Notes

The authors declare no competing financial interest.

ACKNOWLEDGMENTS

Financial support from the MINECO of Spain (Projects CTQ2017-82935-P (AEI/FEDER, UE) and RED2018-102387-T), Gobierno de Aragón (Group E06_17R and project LMP148_18), FEDER, and the European Social Fund is acknowledged. The BIFI Institute and CESGA Supercomputing Center are acknowledged for technical support and the use of computational resources.

REFERENCES

(1) *Pincer Compounds: Chemistry and Applications*, 1st Edition; Morales-Morales, D., Ed.; Elsevier: Amsterdam, 2018.

(2) (a) Williams, J. A. G.; Wilkinson, A. J.; Whittle, V. L. Light-emitting iridium complexes with tridentate ligands. *Dalton Trans.* **2008**, 2081-2099. (b) Chi, Y.; Chang, T.-K.; Ganesan, P.; Rajakannu, P. Emissive bis-tridentate Ir(III) metal complexes: Tactics, photophysics and applications. *Coord. Chem. Rev.* **2017**, *346*, 91-100.

(3) (a) Sauvage, J.-P.; Collin, J.-P.; Chambron, J.-C.; Guillerez, S.; Coudret, C.; Balzani, V.; Barigelletti, F.; De Cola, L.; Flamigni, L. Ruthenium(II) and Osmium(II) Bis(terpyridine) Complexes in Covalently-Linked Multicomponent Systems: Synthesis, Electrochemical Behavior, Absorption Spectra, and Photochemical and Photophysical Properties. *Chem. Rev.* **1994**, *94*, 993-1019. (b) Abrahamsson, M.; Jäger, M.; Kumar, R. J.; Österman, T.; Persson, P.; Becker, H.-C.; Johansson, O.; Hammarström, L. Bistridentate

Ruthenium(II)polypyridyl-Type Complexes with Microsecond ^{3}MLCT State Lifetimes: Sensitizers for Rod-Like Molecular Arrays. *J. Am. Chem. Soc.* **2008**, *130*, 15533-15542.

(4) Baranoff, E.; Collin, J.-P.; Flamigni, L.; Sauvage, J.-P. From ruthenium(II) to iridium(III): 15 years of triads based on bis-terpyridine complexes. *Chem. Soc. Rev.*, **2004**, *33*, 147–155.

(5) (a) Baranoff, E.; Curchod, B. F. E.; Frey, J.; Scopelliti, R.; Kessler, F.; Tavernelli, I.; Rothlisberger, U.; Grätzel, M.; Nazeeruddin, Md. K. Acid-Induced Degradation of Phosphorescent Dopants for OLEDs and Its Application to the Synthesis of Tris-heteroleptic Iridium(III) Bis-cyclometalated Complexes. *Inorg. Chem*. **2012**, *51*, 215-224. (b) Adamovich, V.; Bajo, S.; Boudreault, P.-L.; Esteruelas, M. A.; López, A. M.; Martín, J.; Oliván, M.; Oñate, E.; Palacios, A. U.; San-Torcuato, A.; Tsai, J.-Y.; Xia, C. Preparation of Tris-Heteroleptic Iridium(III) Complexes Containing a Cyclometalated Aryl-N-Heterocyclic Carbene Ligand. *Inorg. Chem*. **2018**, *57*, 10744-10760.

(6) (a) You, Y.; Nam, W. Photofunctional triplet excited states of cyclometalated Ir(III) complexes: beyond electroluminescence. *Chem. Soc. Rev*., **2012**, *41*, 7061–7084. (b) Jou, J.-H.; Kumar, S.; Agrawal, A.; Li, T.-H.; Sahoo, S. Approaches for fabricating high efficiency organic light emitting diodes. *J. Mater. Chem. C,* **2015**, *3*, 2974-3002. (c) Zanoni, K. P. S.; Coppo, R. L.; Amaral, R. C.; Iha, N. Y. M. Ir(III) complexes designed for light-emitting devices: beyond the luminescence color array. *Dalton Trans*. **2015**, *44*, 14559–14573. (d) Henwood, A. F.; Zysman-Colman, E. Lessons learned in tuning the optoelectronic properties of phosphorescent iridium(III) complexes. *Chem. Commun*. **2017**, *53*, 807-826. (e) Li, T.-Y.; Wu, J.; Wu, Z.-G.; Zheng, Y.-X.; Zuo, J.-L; Pan, Y.

Rational design of phosphorescent iridium(III) complexes for emission color tunability and their applications in OLEDs. *Coord. Chem. Rev*. **2018**, *374*, 55–92.

(7) (a) Lalevée, J.; Peter, M.; Dumur, F.; Gigmes, D.; Blanchard, N.; Tehfe, M.-A.; Morlet-Savary, F.; Fouassier, J. P. Subtle Ligand Effects in Oxidative Photocatalysis with Iridium Complexes: Application to Photopolymerization. *Chem. Eur. J*. **2011**, *17*, 15027 – 15031. (b) Prier, C. K.; Rankic, D. A.; MacMillan, D. W. C. Visible Light Photoredox Catalysis with Transition Metal Complexes: Applications in Organic Synthesis. *Chem. Rev*. **2013**, *113*, 5322-5363. (c) Arias-Rotondo, D. M.; McCusker, J. K. The photophysics of photoredox catalysis: a roadmap for catalyst design. *Chem. Soc. Rev.,* **2016**, 5803-5820. (d) Tehfe, M.-A.; Lepeltier, M.; Dumur, F.; Gigmes, D.; Fouassier, J. P.; Lalevée, J. Structural Effects in the Iridium Complex Series: Photoredox Catalysis and Photoinitiation of Polymerization Reactions under Visible Lights. *Macromol. Chem. Phys.* **2017**, *218*, 1700192. (e) Marzo, L.; Pagire, S. K.; Reiser, O.; König, B. Visible-Light Photocatalysis: Does It Make a Difference in Organic Synthesis? *Angew. Chem. Int. Ed.* **2018**, *57*, 10034–10072.

(8) Williams, J. A. G. The coordination chemistry of dipyridylbenzene: N-deficient terpyridine or panacea for brightly luminescent metal complexes? *Chem. Soc. Rev*., **2009**, *38*, 1783–1801.

(9) (a) Barigelletti, F.; Flamigni, L.; Guardigli, M.; Juris, A.; Beley, M.; Chodorowski-Kimmes, S.; Collin, J.-P.; Sauvage, J.-P. Energy Transfer in Rigid Ru(II)/Os(II) Dinuclear Complexes with Biscyclometalating Bridging Ligands Containing a Variable Number of Phenylene Units. *Inorg. Chem*. **1996**, *35*, 136-142. (b) Williams, J. A. G.;

Beeby, A.; Davies, E. S.; Weinstein, J. A.; Wilson, C. An Alternative Route to Highly Luminescent Platinum(II) Complexes: Cyclometalation with N^C^N-Coordinating Dipyridylbenzene Ligands *Inorg. Chem.* **2003**, *42*, 8609-8611.

(10) Wilkinson, A. J.; Goeta, A. E.; Foster, C. E.; Williams, J. A. G. Synthesis and Luminescence of a Charge-Neutral, Cyclometalated Iridium(III) Complex Containing N^C^N- and C^N^C-Coordinating Terdentate Ligands. *Inorg. Chem.* **2004**, *4*3, 6513−6515.

(11) Wilkinson, A. J.; Puschmann, H.; Howard, J. A. K.; Foster, C. E.; Williams, J. A. G. Luminescent Complexes of Iridium(III) Containing N^C^N-Coordinating Terdentate Ligands. *Inorg. Chem.* **2006**, *45*, 8685−8699.

(12) (a) Tong, B.; Ku, H.-Y.; Chen, I.-J.; Chi, Y.; Kao, H.-C.; Yeh, C.-C.; Chang, C.-H.; Liu, S.-H.; Lee, G.-H.; Chou, P.-T. Heteroleptic Ir(III) phosphors with bis-tridentate chelating architecture for high efficiency OLEDs. *J. Mater. Chem. C* **2015**, *3*, 3460−3471. (b) Esteruelas, M. A.; Gómez-Bautista, D.; López, A. M.; Oñate, E.; Tsai, J.-Y.; Xia, C. η^1-Arene Complexes as Intermediates in the Preparation of Molecular Phosphorescent Iridium(III) Complexes. *Chem. - Eur. J.* **2017**, *23*, 15729−15737.

(13) Adamovich, V.; Boudreault, P.-L. T.; Esteruelas, M. A.; Gómez-Bautista, D.; López, A. M.¸ Oñate, E.; Tsai, J.-Y. Preparation via a NHC Dimer Complex, Photophysical Properties, and Device Performance of Heteroleptic Bis(Tridentate) Iridium(III) Emitters. *Organometallics* **2019**, *38*, 2738−2747.

(14) Esteruelas, M. A.; López, A. M.; Oñate, E.; San-Torcuato, A.; Tsai, J.-Y.; Xia, C. Preparation of Phosphorescent Iridium(III) Complexes with a Dianionic C,C,C,C-Tetradentate Ligand. *Inorg. Chem*. **2018**, *57*, 3720–3730.

(15) (a) Kuei, C.-Y.; Tsai, W.-L.; Tong, B.; Jiao, M.; Lee, W.-K.; Chi, Y.; Wu, C.-C.; Liu, S.-H.; Lee, G.-H.; Chou, P.-T. Bis-Tridentate Ir(III) Complexes with Nearly Unitary RGB Phosphorescence and Organic Light-Emitting Diodes with External Quantum Efficiency Exceeding 31%. *Adv. Mater.* **2016**, *28*, 2795–2800. (b) Kuei, C.-Y.; Liu, S.-H.; Chou, P.-T. Lee, G.-H.; Chi, Y. Room temperature blue phosphorescence: a combined experimental and theoretical study on the bis-tridentate Ir(III) metal complexes. *Dalton Trans*. **2016**, *45*, 15364-15373. (c) Kuo, H.-H.; Chen, Y.-T.; Devereux, L. R.; Wu, C.-C.; Fox, M. A.; Kuei, C.-Y.; Chi, Y.; Lee G.-H. Bis-Tridentate Ir(III) Metal Phosphors for Efficient Deep-Blue Organic Light-Emitting Diodes. *Adv. Mater.* **2017**, *29*, 1702464. (d) Kuo, H.-H.; Zhu, Z.-L.; Lee, C.-S.; Chen, Y.-K.; Liu, S.-H.; Chou, P.-T.; Jen, A. K.-Y.; Chi, Y. Bis-Tridentate Iridium(III) Phosphors with Very High Photostability and Fabrication of Blue-Emitting OLEDs. *Adv. Sci.* **2018**, 1800846.

(16) (a) Chen, J.-L.; Wu, Y.-H.; He, L.-H.; Wen, H.-R.; Liao, J.; Hong, R. Iridium(III) Bis-tridentate Complexes with 6-(5-Trifluoromethylpyrazol-3-yl)-2,2'-bipyridine Chelating Ligands: Synthesis, Characterization, Photophysical Properties. *Organometallics* **2010**, *29*, 2882–2891. (b) Lu, C.W.; Wang, Y.; Chi, Y. Metal Complexes with Azolate-Functionalized Multidentate Ligands: Tactical Designs and Optoelectronic Applications. *Chem Eur. J.* **2016**, *22*, 17892-17908. (c) Lin, J.; Chau, N.-Y.; Liao, J.-L.; Wong, W.-Y.; Lu, C.-Y.; Sie, Z.-T.; Chang, C.-H.; Fox, M. A.; Low, P. J.; Lee, G.-H.; Chi, Y. Bis-Tridentate Iridium(III) Phosphors Bearing Functional 2‑Phenyl-6-(imidazol-2-

ylidene)pyridine and 2‑(Pyrazol-3-yl)-6-phenylpyridine Chelates for Efficient OLEDs. *Organometallics* **2016**, *35*, 1813−1824. (d) Lin, J.; Wang, Y.; Gnanasekaran, P.; Chiang, Y.-C.; Yang, C.-C.; Chang, C.-H.; Liu, S.-H.; Lee, G.-H.; Chou, P.-T.; Chi, Y.; Liu, S.-W. Unprecedented Homoleptic Bis-Tridentate Iridium(III) Phosphors: Facile, Scaled-Up Production, and Superior Chemical Stability. *Adv. Funct. Mater.* **2017**, *27*, 1702856.

(17) Kim, J.-H.; Kim, S.-Y.; Cho, D. W.; Son, H.-J.; Kang, S. O. Influence of bulky substituents on the photophysical properties of homoleptic iridium(III) complexes. *Phys. Chem. Chem. Phys.* **2019**, *21*, 6908−6916.

(18) Alabau, R. G.; Esteruelas, M. A.; Oliván, M.; Oñate, E. Preparation of Phosphorescent Osmium(IV) Complexes with N,N′,C and C,N,C′-Pincer Ligands. *Organometallics* **2017**, *36*, 1848−1859.

(19) Cárdenas, D.; Echavarren, A. M. Divergent Behavior of Palladium(II) and Platinum(II) in the Metalation of 1,3-Di(2-pyridyl)benzene. *Organometallics* **1999,** *18,* 3337-3341.

(20) Soro, B.; Stoccoro, S.; Minghetti, G.; Zucca, A.; Cinellu, M. A.; Gladiali, S.; Manassero, M.; Sansoni, M. Synthesis of the First C-2 Cyclopalladated Derivatives of 1,3-Bis(2-pyridyl)benzene. Crystal Structures of [Hg(N-C-N)Cl], [Pd(N-C-N)Cl], and $[Pd_2(N\text{-}C\text{-}N)_2(\mu\text{-}OAc)]_2[Hg_2Cl_6]$. Catalytic Activity in the Heck Reaction. *Organometallics* **2005**, *24,* 53-61.

(21) Calligaris, M. Structure and bonding in metal sulfoxide complexes: an update. *Coord. Chem. Rev*. **2004**, *248*, 351-375.

(22) (a) Böttcher, H.-C.; Graf, M.; Sünkel, K.; Mayer, P.; Krüger, H. [Ir(acac)(η^2-C_8H_{14})$_2$]: A precursor in the synthesis of cyclometalated iridium(III) complexes. *Inorg. Chim. Acta* **2011**, *365*, 103–107. (b) Boudreault, P.-L.; Esteruelas, M. A.; Mora, E.; Oñate, E.; Tsai, J.-Y. Pyridyl-Directed C–H and C–Br Bond Activations Promoted by Dimer Iridium-Olefin Complexes. *Organometallics* **2018**, *37*, 3770–3779.

(23) Esteruelas, M. A.; López, A. M.; Oliván, M. Polyhydrides of Platinum Group Metals: Nonclassical Interactions and σ‑Bond Activation Reactions. *Chem. Rev*. **2016**, *116*, 8770–8847.

(24) Complexes **4**–**7** exhibit a second oxidation peak at higher potentials (0.78–0.87 V).

(25) Castro-Rodrigo, R.; Esteruelas, M. A.; Gómez-Bautista, D.; Lezáun, V.; López, A. M.; Oliván, M.; Oñate, E. Influence of the Bite Angle of Dianionic C,N,C-Pincer Ligands on the Chemical and Photophysical properties od Iridium(III) and Osmium(IV) Hydride Complexes. *Organometallics* **2019**, *38*, 3707-3718.

(26) (a) Shi, C.; Pan, J.; Yan, X. Organometallic complex, high polymer, mixture, composition and organic electronic device. WO2017/092481A1, 2017. (b) Boudreault, P.-L. T.; Esteruelas, M. A.; Mora, E.; Oñate, E.; Tsai, J.-Y. Suzuki–Miyaura Cross-Coupling Reactions for Increasing the Efficiency of Tris-Heteroleptic Iridium(III) Emitters. *Organometallics* **2019**, *38*, 2883–2887.

(27) van der Ent, A.; Onderdelinden, A. L.; Schunn, R. A. Chlorobis(cyclooctene)rhodium(I) and -iridium(I) complexes. *Inorg. Synth*. **2007**, *28*, 90–92.

(28) Due to the potential toxicity of mercury species, they should be handled very carefully: Breitinger, D. K. Mercury and its Compounds. In *Synthetic Methods of Organometallic and Inorganic Chemistry*; Herrman W. A., Ed.; Thieme: Stutgart, 1999; Vol. 5, Chapter 6, pp 194-195.

(29) Ho, Y.-M.; Koo, C.-K.; Wong, K.-L.; Kong, H.-K.; Chan, C. T.-L.; Kwok, W.-M.; Chow, C.-F.; Lam, M. H.-W.; Wong, W.-Y. The synthesis and photophysical studies of cyclometalated Pt(II) complexes with C,N,N-ligands containing imidazolyl donors. *Dalton Trans*. **2012**, *41*, 1792–1800.

(30) Fu, L.; Pan, M.; Li, Y.-H.; Wu, H.-B.; Wang, H.-P.; Yan, C.; Li, K.; Wei, S.-C.; Wang, Z.; Su, C.-Y. A butterfly-like yellow luminescent Ir(III) complex and its application in highly efficient polymer light-emitting devices. *J. Mater. Chem.* **2012**, *22*, 22496–22500.

(31) Labrière, C.; Gong, H.; Finlay, B. B.; Reiner, N. E.; Young, R. N. Further investigation of inhibitors of MRSA pyruvate kinase: Towards the conception of novel antimicrobial agents. *Eur. J. Med. Chem.* **2017**, *125*, 1-13.

(32) T_d represents the temperature at which the 5% weigh is lost in TGA analysis.

SYNOPSIS

A method to coordinate 2,6-di(2-pyridyl)phenyl to iridium(III) as a N,C,N-pincer ligand (5t) has been developed. Taking advantage of this, new *bis*(tridentate) molecular emitters [5t + 4t'] of iridium(III) have been prepared and their photophysical properties have been studied and compared with those of their counterparts containing the related 5t ligand 2,6-di(2-pyridyl)-3,5-dimethylphenyl, which are also synthetized.

TOC graphic